

Possibilities of production of transfermium nuclei in complete fusion reactions with radioactive beams

Juhee Hong

Rare Isotope Science Project, Institute for Basic Science, Daejeon 34047, Korea

G. G. Adamian

Joint Institute for Nuclear Research, Dubna 141980, Russia

N. V. Antonenko

Joint Institute for Nuclear Research, Dubna 141980, Russia

and Mathematical Physics Department, Tomsk Polytechnic University, 634050 Tomsk, Russia

(Received 24 May 2017; published 13 July 2017)

The possibilities of direct production of new isotopes of transfermium nuclei $^{261,263,264}\text{No}$, $^{263,264}\text{Lr}$, $^{263,264,266,268}\text{Rf}$, $^{264,265}\text{Db}$, and $^{267,268,270,272}\text{Sg}$ are studied in various asymmetric hot fusion-evaporation reactions with radioactive beams. The optimal reaction partners and conditions for the synthesis of new isotopes are suggested. The products of the suggested reactions can fill a gap of unknown isotopes between the isotopes of heaviest nuclei obtained in the xn evaporation channels of the cold and hot complete fusion reactions with the stable beams.

DOI: [10.1103/PhysRevC.96.014609](https://doi.org/10.1103/PhysRevC.96.014609)

I. INTRODUCTION

The hot actinide-based and cold ^{208}Pb - and ^{209}Bi -based complete fusion reactions have been intensively and successfully used to produce heavy and superheavy nuclei in the neutron-evaporation channels (xn channels) [1–15]. However, the synthesis of different isotopes of heaviest nuclei with the charge numbers $Z = 103$ – 108 in these reaction channels is limited by the number of available stable projectiles and targets and the small production cross sections. There is a gap of unknown isotopes ($Z = 103$ – 108) between the neutron-deficient superheavy nuclei obtained in cold fusion and the heaviest isotopes formed in hot fusion.

As demonstrated in Ref. [16], with asymmetry-exit-channel quasifission (multinucleon transfer [17–22]) reactions $^{48}\text{Ca} + ^{244,246,248}\text{Cm}$ at energies near the corresponding Coulomb barriers one can produce new isotopes with charge numbers $Z = 103$ – 108 . New isotopes of heaviest nuclei can also be synthesized with stable beams in the asymmetric actinide-based complete fusion-evaporation reactions with the emission of charged particles from the compound nucleus (CN) [23,24]. However, there is an other possibility of the direct production of some unknown heaviest isotopes in the complete fusion reactions with the actinide-targets and the radioactive beams. Although the intensities of radioactive beams are presently much smaller than those of stable beams, they can be used if the production rate of the isotope of interest is suitable for existing experimental setups. In the present article we focus on this possibility considering the neutron and charged particle evaporation channels. For unknown isotopes of nuclei with $Z = 102$ – 106 , we make predictions of the production cross sections and indicate the optimal reactions for producing new isotopes. The prospects for the synthesis of transactinide nuclei in the xn channels using radioactive beams have been already discussed in Refs. [25–27]. The emission of charged particles competes with the neutron evaporation and fission. For the

excited heavy nucleus, the emission of charged particles is suppressed by the high Coulomb barrier. However, if after emission of charged particles the daughter nucleus has higher fission barrier than the parent nucleus, the survival probability can be relatively large and one can obtain new isotopes of transfermium nuclei with relatively large cross section.

II. MODEL

In the excited superheavy nucleus (SHN), the emission of charged particles is suppressed by the high Coulomb barrier and competes with the neutron evaporation and fission. The evaporation residue cross section [28–39]

$$\sigma_s(E_{c.m.}) = \sum_{J=0} \sigma_{\text{cap}}(E_{c.m.}, J) P_{\text{CN}}(E_{c.m.}, J) W_s(E_{c.m.}, J) \quad (1)$$

in the evaporation channel s depends on the partial capture cross section σ_{cap} for the transition of the colliding nuclei over the entrance (Coulomb) barrier, the probability of CN formation P_{CN} after the capture and the survival probability W_s of the excited CN. The formation of CN is described within the dinuclear system (DNS) model [24]. In the first step of a fusion reaction the projectile is captured by the target. In the second step a formed DNS evolves into the CN in the mass asymmetry coordinate $\eta = (A_1 - A_2)/(A_1 + A_2)$ (A_1 and A_2 are the mass numbers of the DNS nuclei) [28–35,37,38]. Since the bombarding energy $E_{c.m.}$ of the projectile is usually higher than the Q value for the CN formation, the produced nucleus is excited. In the third step of the reaction the CN loses its excitation energy mainly by the emission of particles and γ quanta [40–47]. In the deexcitation of a CN, the charged particle emission competes with the fission and neutron emission. We describe the production of nuclei in the evaporation channels with emission of charged particle (proton or α particle) and neutrons as in Ref. [24]. The emissions of other particles are assumed to be negligible

to contribute to the total width of the CN decay [36]. The deexcitation of the CN is treated with the statistical model using the level densities from the Fermi-gas model. The neutron B_n , proton B_p , and α particle B_α binding energies, the nuclear mass excesses of superheavy nuclei, and the ground-state microscopic corrections (their absolute values are approximately equal to the fission barriers for the nuclei considered) are taken from Ref. [48]. With the level-density parameter $a_n = a = A/10 \text{ MeV}^{-1}$ for neutron (A is the mass number of the CN), the level-density parameters for fission, proton-emission, and α -emission channels are taken as $a_f = 1.04a$, $a_p = 0.96a$, and $a_\alpha = 1.15a$, respectively. For the calculation of the Coulomb barrier, we use the expression

$$V_j = \frac{(Z - z_j)z_j e^2}{r_j[(A - m_j)^{1/3} + m_j^{1/3}]}, \quad (2)$$

where z_j (m_j) are the charge (mass) numbers of the charged particle (proton or α particle) and r_j is a constant. The charge Z (mass A) number corresponds to the CN. There are different theoretical estimations of r_j [40,47]. In the case of α emission, r_α varies from 1.3 to 1.78 fm. We obtain r_α from the energy

of the DNS formed by the daughter nucleus and α particle. We calculate the Coulomb barrier in the interaction potential between the α particle and the daughter nucleus [49], and find the value of r_α from Eq. (2). For different nuclei considered, we obtained $r_\alpha = 1.57 \text{ fm}$ using this method. Thus, in the calculations of V_α we set $r_\alpha = 1.57 \text{ fm}$ for nuclei considered. The parameter r_p for the Coulomb barrier for proton emission is taken as $r_p = 1.7 \text{ fm}$ from Refs. [37,47]. As seen, the values of σ_s near the maximum are almost insensitive to the variations of this parameter, but far from the maximum they change up to one order of magnitude. We would like to stress the weak dependence of the calculated σ_s near the maxima of the excitation functions on the reasonable variation of all parameters discussed. Therefore, the results obtained in this paper have quite a small uncertainty near the maxima of the excitation functions which are important to obtain the largest yield of certain nucleus in the experiments. We estimate this uncertainty within a factor of 2–4. Our calculations are tested for many known reactions in which the excitation functions of transfermium nuclei produced in the charged particle evaporation channels have been measured [24].

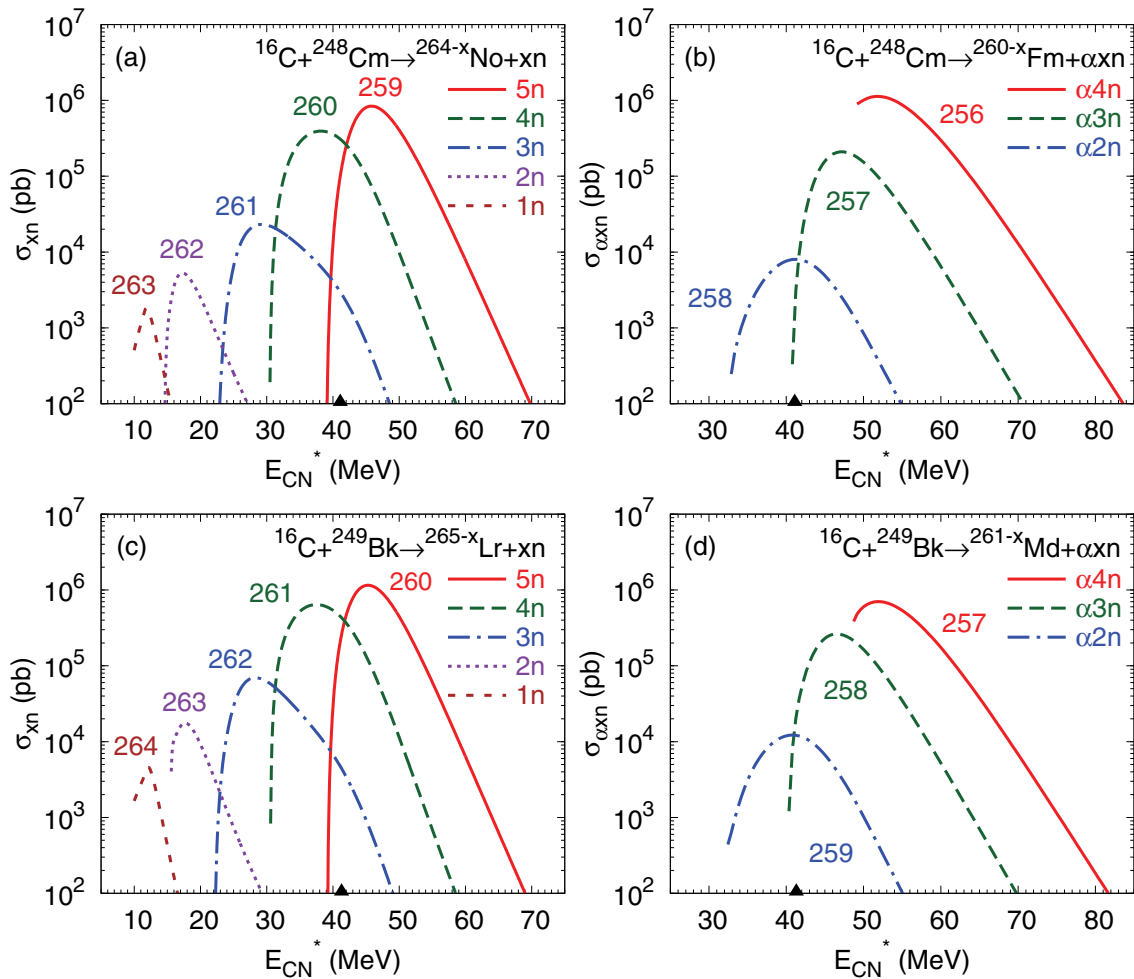


FIG. 1. The measured (symbols) and calculated (lines) excitation functions for xn and αxn evaporation channels in the indicated reactions with ^{16}C beam. The mass table of Ref. [48] is used in the calculations. The black triangles at the energy axis indicate the excitation energy $E_{\text{CN}}^* = V_b + Q$ of the CN where V_b is the Coulomb barrier for spherical nuclei.

The fission barrier B_f has the liquid-drop B_f^{LD} [50] and microscopic $B_f^M(E_{CN}^*)$ parts: $B_f(E_{CN}^*) = B_f^{LD} + B_f^M(E_{CN}^*)$. For the considered isotopes of nuclei with $Z = 102-106$, B_f^{LD} is in the energy range of 1.6–3.7 MeV. The value $B_f^M = \delta W_{sd} - \delta W_{gr}$ is the difference between the shell correction δW_{sd} of nucleus at the saddle point and the shell correction δW_{gr} of nucleus in the ground state. Usually, one neglects the shell correction at the saddle point, $\delta W_{sd} \approx 0$ and, thus, $B_f^M = |\delta W_{gr}|$. Due to the dependence of the shell effects on the nuclear excitation, the value of B_f effectively depends on E_{CN}^* as

$$B_f(E_{CN}^*) = B_f^{LD} + B_f(E_{CN}^* = 0) \exp[-E_{CN}^*/E_d],$$

where the damping factor is $E_d = 25$ MeV. The pairing corrections $\Delta = 22/\sqrt{A}$, $11/\sqrt{A}$, and 0 for even-even, even-odd, and odd-odd nuclei, respectively, are regarded as follows: $E_{CN}^* - B_j \rightarrow E_{CN}^* - B_j - \Delta$, where $j = n, p, \alpha, f$, in the level densities. The neutron binding energies B_n and the microscopic corrections δW_{gr}^{mc} are taken from Ref. [48]. To avoid a double counting of pairing in the fission barrier which is purely the shell correction, $B_f^M = |\delta W_{gr}| \approx |\delta W_{gr}^{mc}| - \Delta$.

III. CALCULATED RESULTS

The fusion model discussed in Sec. II is used to calculate the excitation functions in various reactions with radioactive beams (Figs. 1–10). In the asymmetric actinide-based reactions with beams of ^{16}C , $^{20,21}\text{O}$, $^{21,23}\text{F}$, $^{24-26}\text{Ne}$, the fusion probability P_{CN} is almost equal to 1. In the reactions $^{24,25,27}\text{Na}$, $^{28,30}\text{Mg} + ^{244}\text{Pu}$, and $^{28}\text{Mg} + ^{238}\text{U}$, $P_{CN} \approx (0.3-0.9)$. Therefore, in these reactions the value of cross section is mainly determined by the survival probability in the xn or αxn evaporation channel and the capture cross section at subbarrier energies. The reactions considered look unfavorable for the pxn channels due to the smaller cross sections.

A. Production of $^{258-264}\text{No}$

The isotopes $^{258-264}\text{No}$ can be produced in the xn and/or αxn evaporation channels of the complete fusion reactions $^{16}\text{C} + ^{248}\text{Cm} \rightarrow ^{264}\text{No}^*$ [Fig. 1(a)], $^{20,21}\text{O} + ^{244}\text{Pu} \rightarrow ^{264,265}\text{No}^*$ [Figs. 2(a) and 2(c)], $^{20,21}\text{O} + ^{248}\text{Cm} \rightarrow ^{268,269}\text{Rf}^*$ [Figs. 3(a) and 3(c)], and $^{28}\text{Mg} + ^{238}\text{U} \rightarrow ^{266}\text{Rf}^*$ [Fig. 4(b)]. The isotopes $^{261,263,264}\text{No}$ are unknown yet. Among various reactions considered above, the reactions $^{16}\text{C} + ^{248}\text{Cm} \rightarrow$

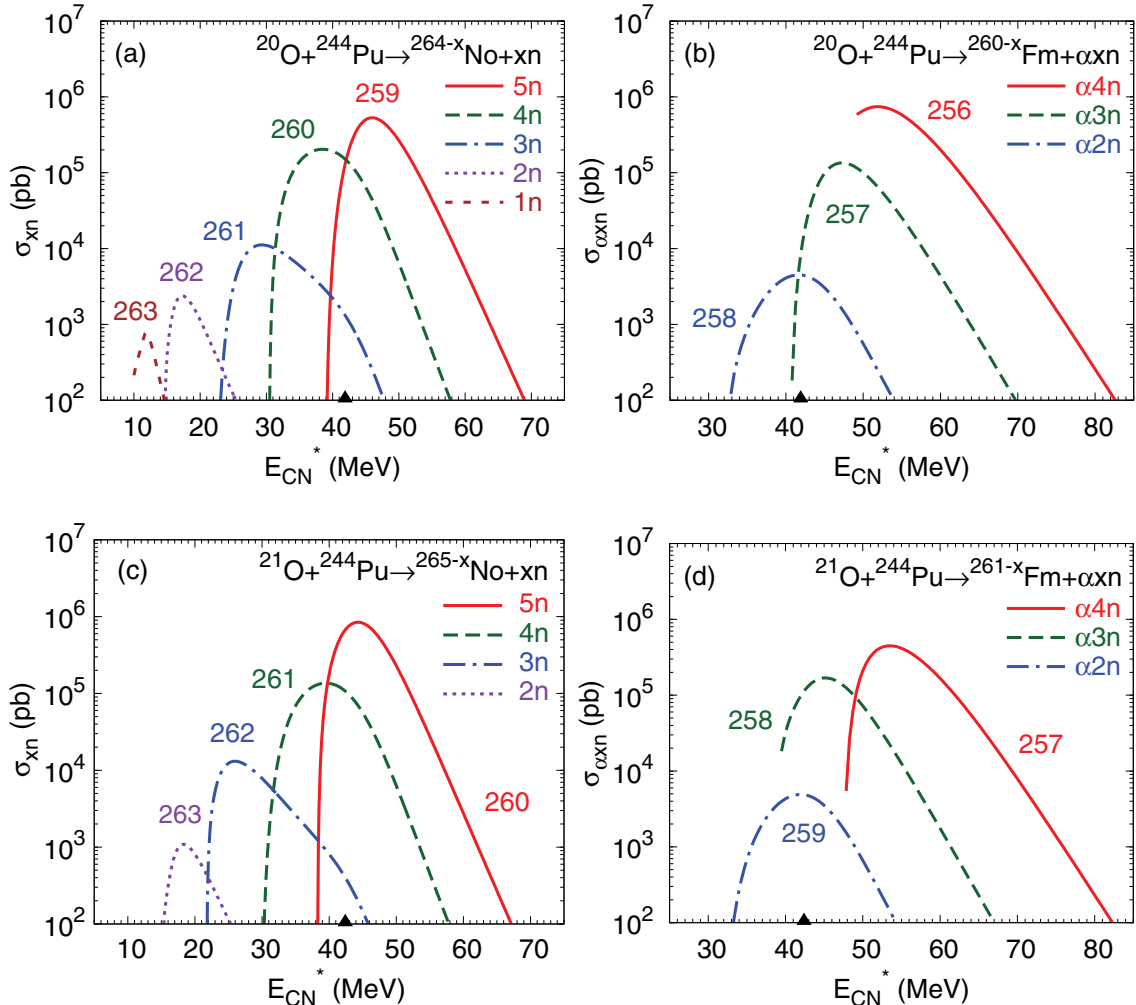
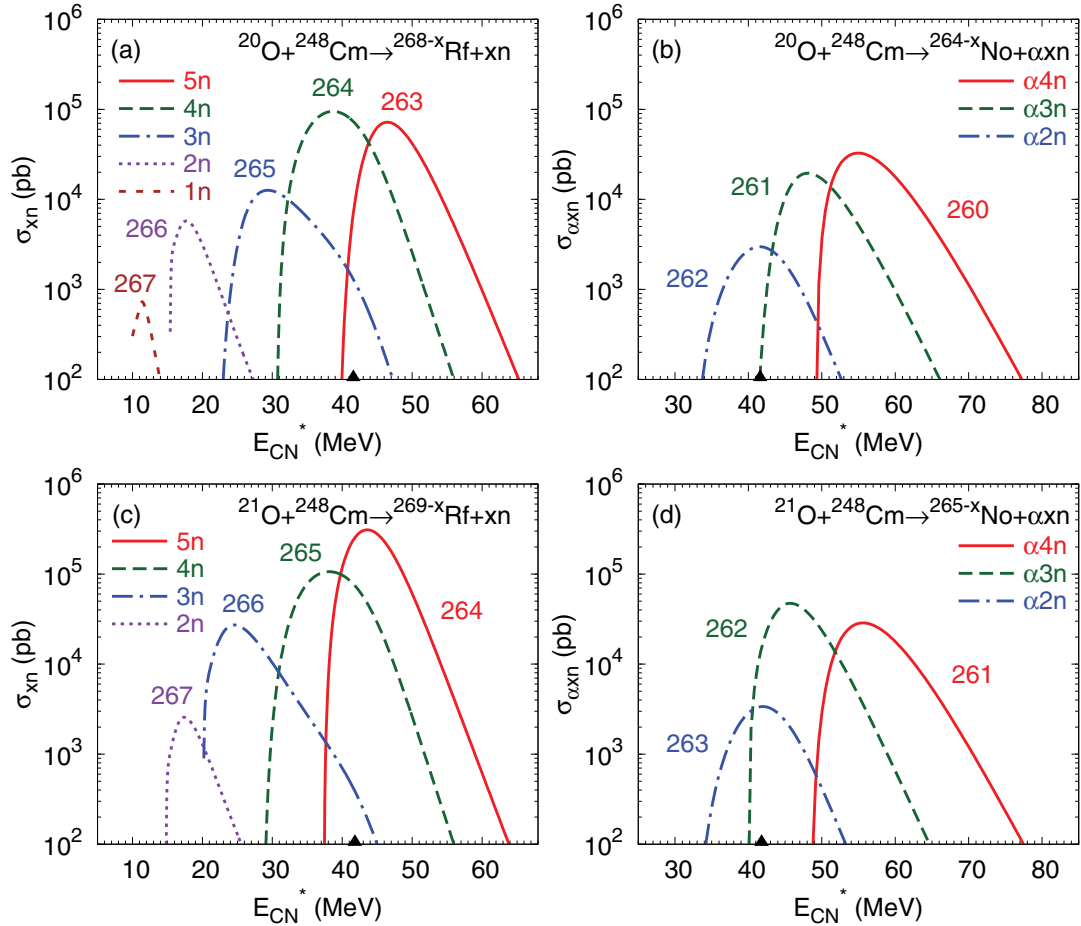


FIG. 2. The same as in Fig. 1, but for the indicated reactions with $^{20,21}\text{O}$ beams.


 FIG. 3. The same as in Fig. 1, but for the indicated reactions with $^{20,21}\text{O}$ beams.

$^{261}\text{No} + 3n$ and $^{20,21}\text{O} + ^{248}\text{Cm} \rightarrow ^{261}\text{No} + \alpha 3n, \alpha 4n$ seem to be the most suitable for the synthesis of ^{261}No with the maximum cross sections $\sigma_{3n} = 23$ nb, $\sigma_{\alpha 3n} = 20$ nb, and $\sigma_{\alpha 4n} = 44$ nb, respectively (Table I). Because the $3n$ -channel peak is under the barrier, the calculated capture cross section in this channel is significantly smaller than that in the $\alpha 3n$ or $\alpha 4n$ channels. In the $^{16}\text{C} + ^{248}\text{Cm}$ reaction, the relatively lower effective capture probability is compensated by the larger survival probability. By employing the reactions $^{16}\text{C} + ^{248}\text{Cm} \rightarrow ^{263}\text{No} + 1n$ and $^{20,21}\text{O} + ^{248}\text{Cm} \rightarrow ^{263}\text{No} + 1n, 2n$, one can also produce the isotopes ^{263}No with the maximum production cross sections about 1–2 nb. Note that new isotope ^{264}No can be produced in the $^{21}\text{O} + ^{244}\text{Pu} \rightarrow ^{264}\text{No} + 1n$ reaction with the maximum cross section of 1 nb.

B. Production of $^{260-265}\text{Lr}$

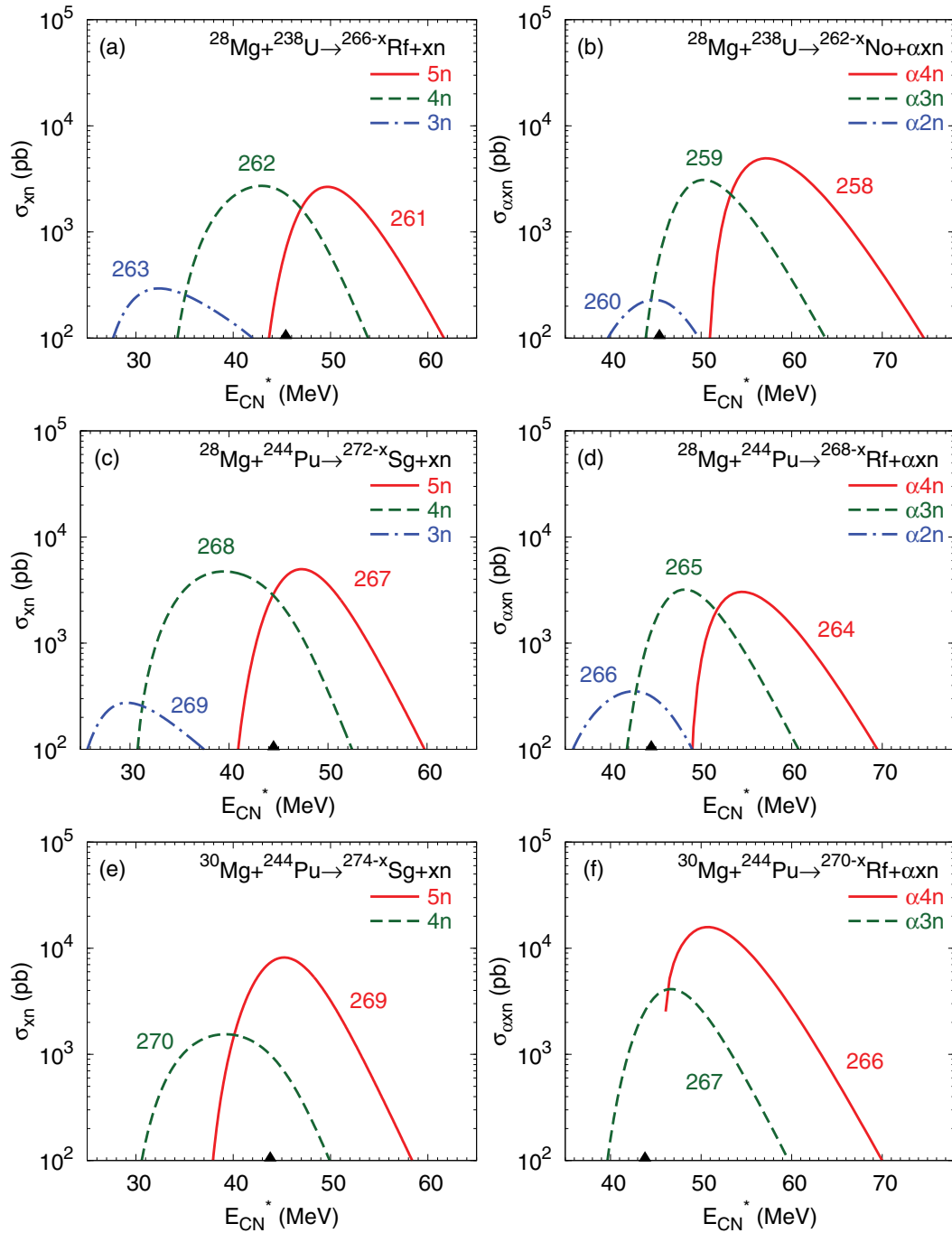
Figures 1 and 5–7 show the calculated excitation functions for the xn and/or αxn evaporation channels in the reactions with the radioactive beams ^{16}C , $^{20,21}\text{O}$, $^{21,23}\text{F}$, and $^{24,25,27}\text{Na}$. The reactions $^{21}\text{O} + ^{249}\text{Bk} \rightarrow ^{263}\text{Lr} + \alpha 3n$ [$\sigma_{\alpha 3n}(^{263}\text{Lr}) = 140$ nb], $^{27}\text{Na} + ^{244}\text{Pu} \rightarrow ^{263}\text{Lr} + \alpha 4n$ [$\sigma_{\alpha 4n}(^{263}\text{Lr}) = 88$ nb], and $^{23}\text{F} + ^{248}\text{Cm} \rightarrow ^{263,264,265}\text{Lr} + \alpha 4n, \alpha 3n, \alpha 2n$ [$\sigma_{\alpha 4n}(^{263}\text{Lr}) = 270$ nb, $\sigma_{\alpha 3n}(^{264}\text{Lr}) = 110$ nb, $\sigma_{\alpha 2n}(^{265}\text{Lr}) = 3.7$ nb] are preferable for producing still unknown isotopes $^{263-265}\text{Lr}$.

C. Production of $^{261-268}\text{Rf}$

The isotopes $^{261-268}\text{Rf}$ ($^{263,264,266,268}\text{Rf}$ are presently unknown) can be produced in the xn channels of the reactions $^{20,21}\text{O} + ^{248}\text{Cm}$ [Figs. 3(a) and 3(c)], $^{28}\text{Mg} + ^{238}\text{U}$ [Fig. 4(a)] and in the αxn channels of the reactions $^{28,30}\text{Mg} + ^{244}\text{Pu}$ [Figs. 4(d) and 4(f)], $^{20,21}\text{O} + ^{251}\text{Cf}$ [Figs. 8(b) and 8(d)], $^{21}\text{O} + ^{249,250}\text{Cf}$ [Figs. 9(b) and 9(d)], $^{24-26}\text{Ne} + ^{248}\text{Cm}$ [Figs. 10(b), 10(d), and 10(f)]. The reactions $^{20,21}\text{O} + ^{248}\text{Cm}$ seem to be optimal for the synthesis of the isotopes $^{263,264,266,268}\text{Rf}$ in the neutron evaporation channels where the maximum production cross sections of isotopes $^{263,264,266,268}\text{Rf}$ are 72, 95 or 310, 27, 1.7 nb, respectively (see Table I). The cross sections of the αxn channels in the reactions $^{25}\text{Ne} + ^{248}\text{Cm} \rightarrow ^{266}\text{Rf} + \alpha 3n$, $^{26}\text{Ne} + ^{248}\text{Cm} \rightarrow ^{266}\text{Rf} + \alpha 4n$, and $^{30}\text{Mg} + ^{244}\text{Pu} \rightarrow ^{266}\text{Rf} + \alpha 4n$ are 40, 59, and 16 nb, respectively. In these reactions the discrepancies of the cross sections are mainly attributed to the difference of capture cross sections.

D. Production of $^{263-270}\text{Db}$

In Figs. 5(a) 5(c), 6(a), 6(c), 7(a), 7(c), and 7(e) the calculated excitation functions for the isotopes $^{263-270}\text{Db}$ ($^{264,265,269}\text{Db}$ are still unknown) are shown for xn evaporation


 FIG. 4. The same as in Fig. 1, but for the indicated reactions with $^{28,30}\text{Mg}$ beams.

channels of the reactions $^{20,21}\text{O} + ^{248}\text{Bk}$, $^{21,23}\text{F} + ^{248}\text{Cm}$, and $^{25}\text{Na} + ^{244}\text{Pu}$.

The reactions $^{20}\text{O} + ^{249}\text{Bk} \rightarrow ^{264,265}\text{Db} + 5n, 4n$, $^{21}\text{O} + ^{249}\text{Bk} \rightarrow ^{265}\text{Db} + 5n$, and $^{23}\text{F} + ^{248}\text{Cm} \rightarrow ^{269}\text{Db} + 2n$ are preferable for producing new isotopes $^{264,265,269}\text{Db}$ [$\sigma_{5n}(^{264}\text{Db}) = 72$ nb, $\sigma_{4n}(^{265}\text{Db}) = 160$ nb, $\sigma_{5n}(^{265}\text{Db}) = 300$ nb, $\sigma_{2n}(^{269}\text{Db}) = 2.2$ nb]. The isotopes $^{266,267,268}\text{Db}$ can be produced in the reactions $^{23}\text{F} + ^{248}\text{Cm} \rightarrow ^{266,267,268}\text{Db} + (3-5)n$ with the maximum cross sections of about 300, 150, and 10 nb, respectively.

E. Production of $^{265-272}\text{Sg}$

One can obtain isotopes $^{265-272}\text{Sg}$ in the xn channels ($x = 2-5$) of the reactions $^{20,21}\text{O} + ^{251}\text{Cf}$ [Figs. 8(a) and 8(c)], $^{21}\text{O} + ^{249,250}\text{Cf}$ [Figs. 9(a) and 9(c)], and $^{24-26}\text{Ne} + ^{248}\text{Cm}$ [Figs. 10(a), 10(c), and 10(e), Table I]. As seen in Figs. 8(c) and 10(a), the value of the maximum of the production cross section increases with excitation energy up to the $E_{\text{CN}}^* \approx V_b + Q$ and then decreases. Thus, the strong decrease of the survival probability with increasing energy under the barrier is overcompensated by the increase of the capture probability.

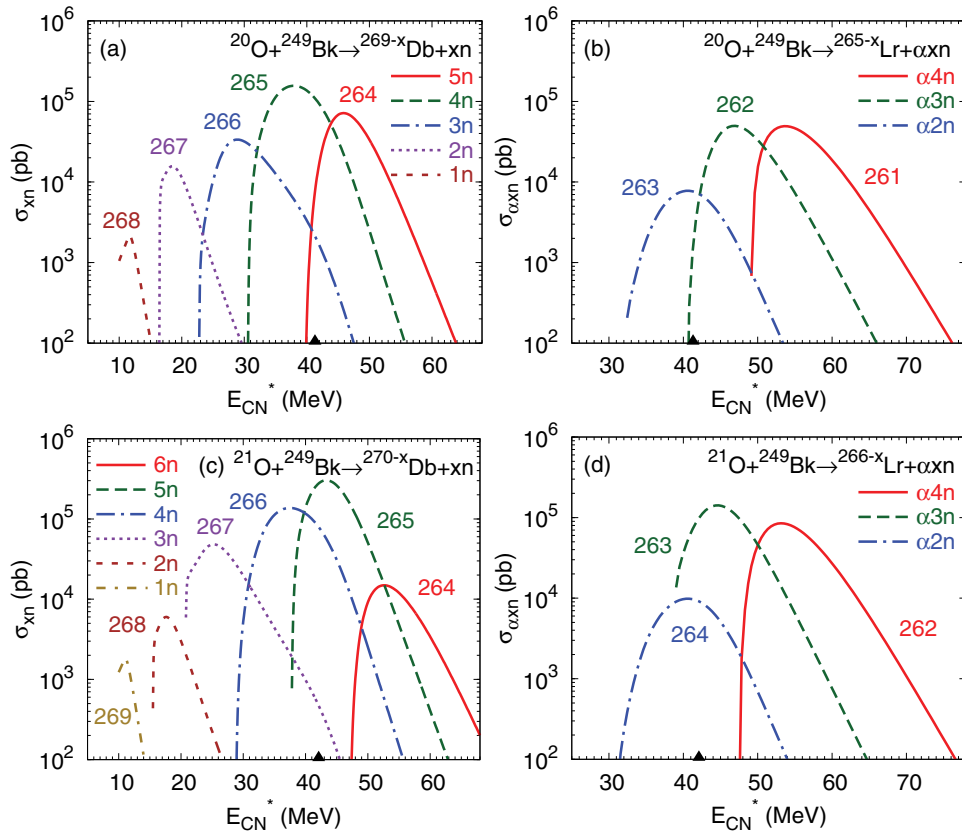


FIG. 5. The same as in Fig. 1, but for the indicated reactions with $^{20,21}\text{O}$ beams.

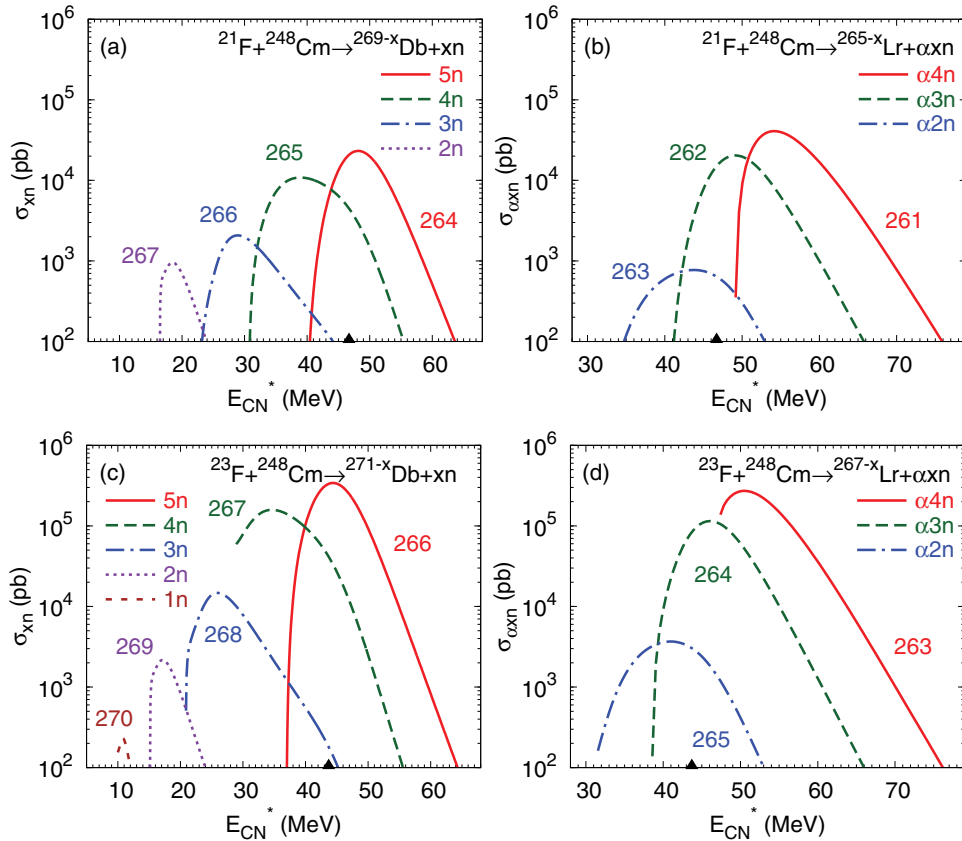


FIG. 6. The same as in Fig. 1, but for the indicated reactions with $^{21,23}\text{F}$ beams.

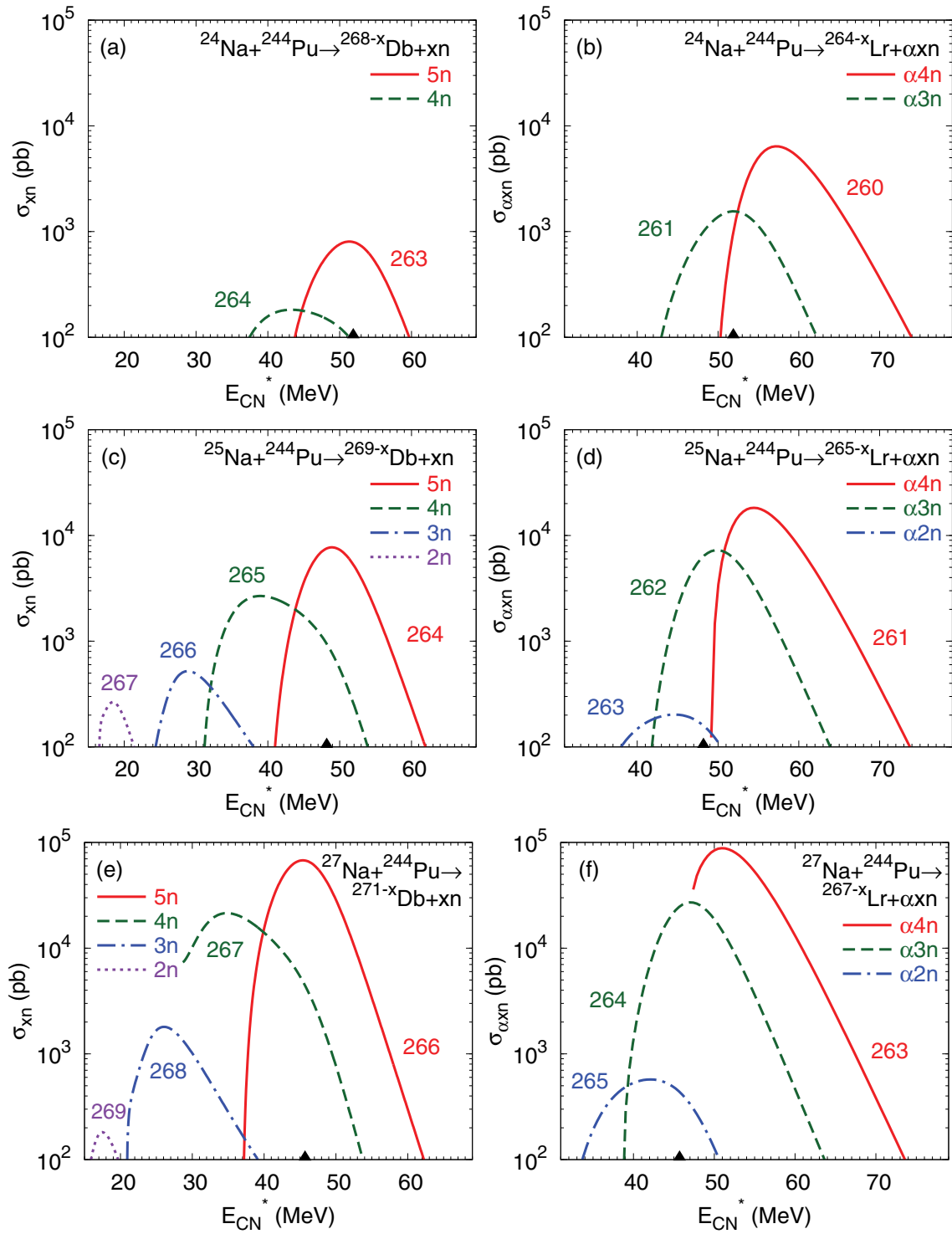


FIG. 7. The same as in Fig. 1, but for the indicated reactions with $^{24,25,27}\text{Na}$ beams.

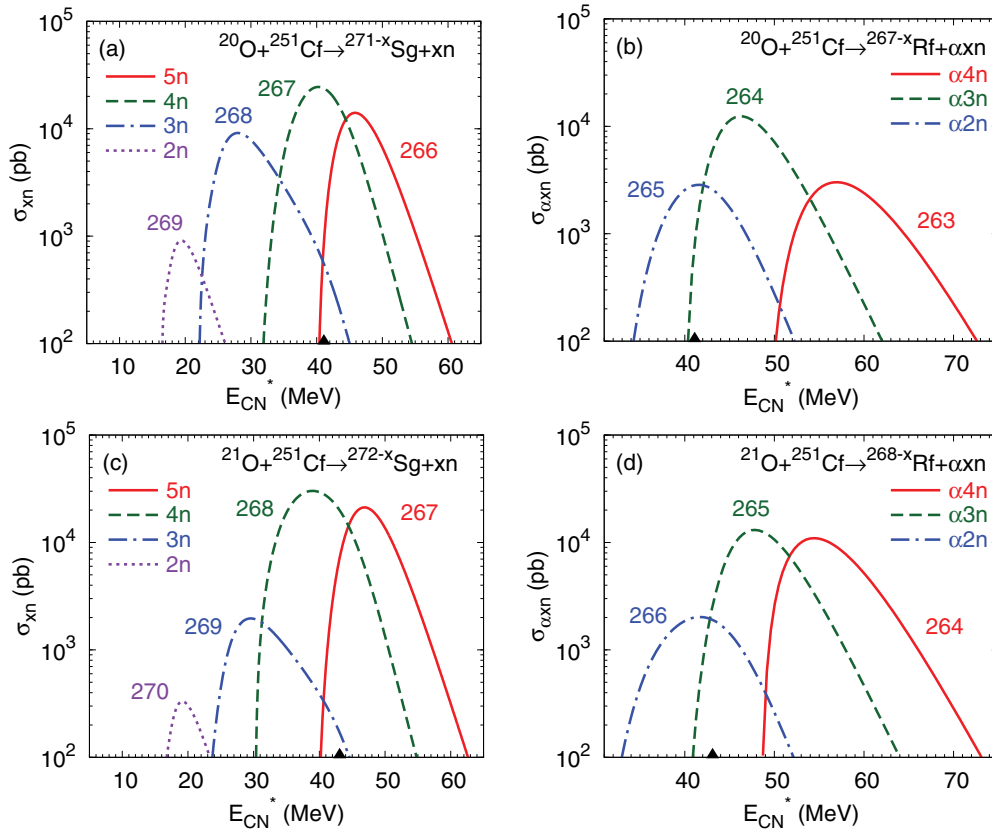


FIG. 8. The same as in Fig. 1, but for the indicated reactions with $^{20,21}\text{O}$ beams.

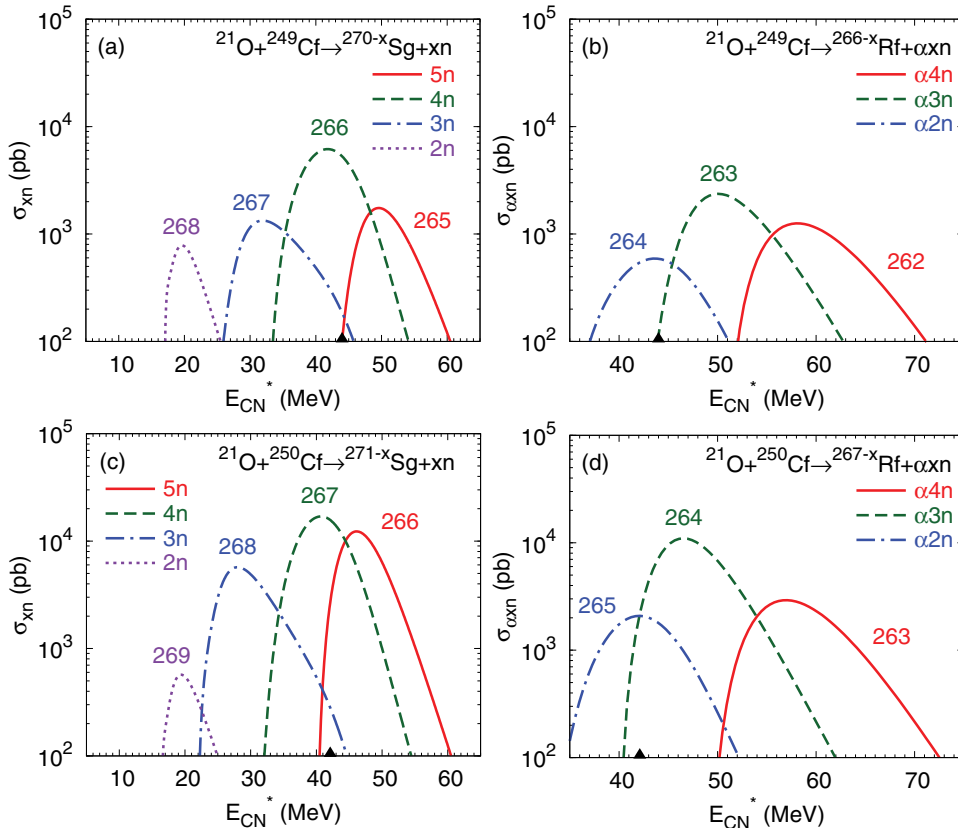


FIG. 9. The same as in Fig. 1, but for the indicated reactions with ^{21}O beams.

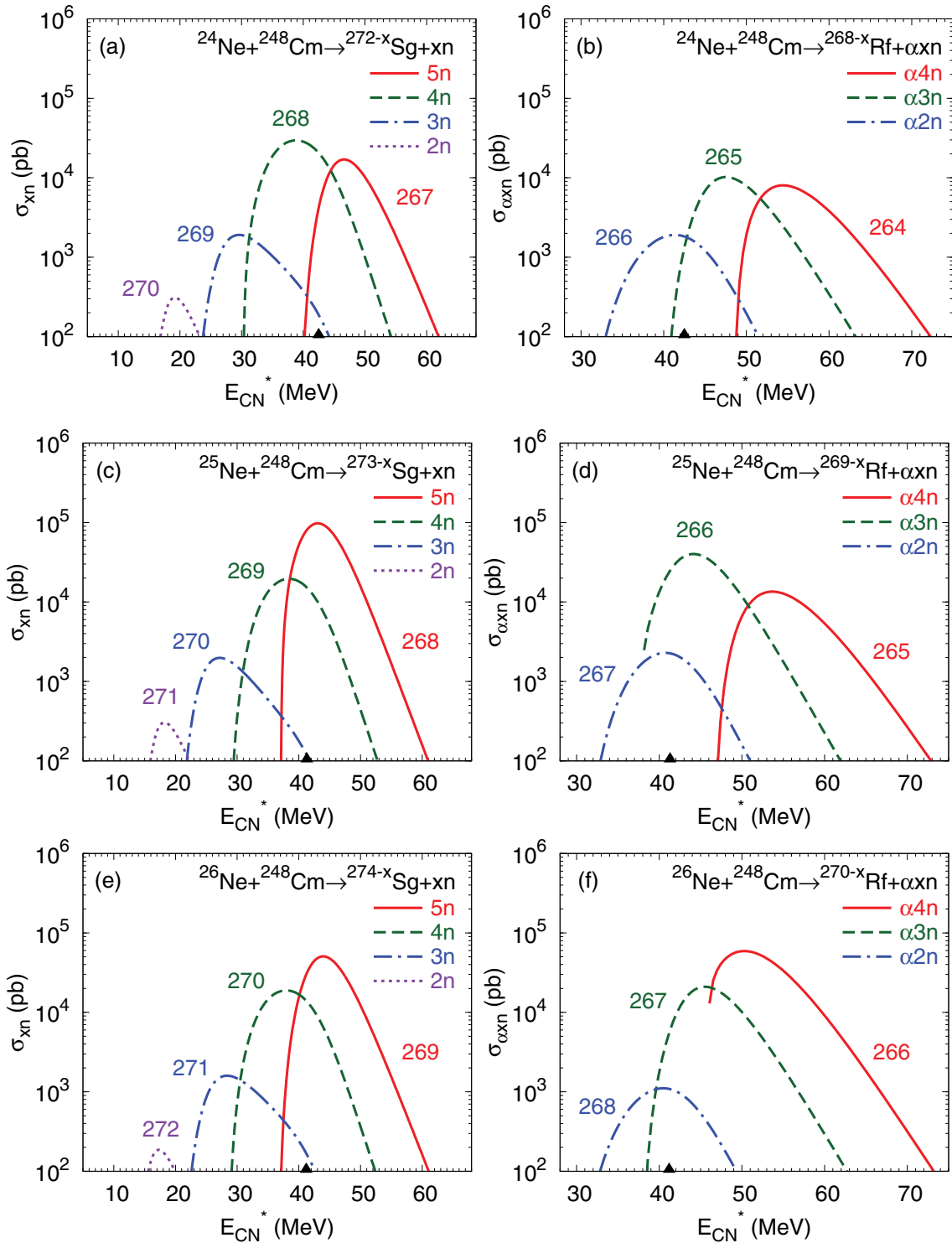


FIG. 10. The same as in Fig. 1, but for the indicated reactions with $^{21,23}\text{F}$ beams.

TABLE I. The calculated evaporation residue cross sections σ_i in the indicated evaporation channels i in various reactions.

Reaction	E_{CN}^* (MeV)	σ_{cap}^{eff} (mb)	W_i	σ_i (nb)
$^{16}\text{C} + ^{248}\text{Cm} \rightarrow ^{261}\text{No} + 3n$	29.2	7.2×10^{-2}	3.2×10^{-4}	23
$^{20}\text{O} + ^{248}\text{Cm} \rightarrow ^{261}\text{No} + \alpha 3n$	48.3	34.5	5.7×10^{-7}	20
$^{21}\text{O} + ^{248}\text{Cm} \rightarrow ^{261}\text{No} + \alpha 4n$	54.4	34.7	1.6×10^{-6}	44
$^{16}\text{C} + ^{248}\text{Cm} \rightarrow ^{263}\text{No} + 1n$	11.8	1.8×10^{-5}	10^{-1}	1.8
$^{20}\text{O} + ^{244}\text{Pu} \rightarrow ^{263}\text{No} + 1n$	11.8	7.7×10^{-6}	10^{-1}	0.8
$^{21}\text{O} + ^{244}\text{Pu} \rightarrow ^{263}\text{No} + 2n$	18.3	1.4×10^{-4}	7.7×10^{-3}	1.1
$^{21}\text{O} + ^{244}\text{Pu} \rightarrow ^{264}\text{No} + 1n$	12.1	7.1×10^{-6}	1.4×10^{-1}	1
$^{16}\text{C} + ^{249}\text{Bk} \rightarrow ^{263}\text{Lr} + 2n$	17.7	2.7×10^{-2}	6.5×10^{-2}	18
$^{21}\text{O} + ^{249}\text{Bk} \rightarrow ^{263}\text{Lr} + \alpha 3n$	44.8	21.6	6.6×10^{-6}	140
$^{23}\text{F} + ^{248}\text{Cm} \rightarrow ^{263}\text{Lr} + \alpha 4n$	50.5	27.4	9.9×10^{-6}	270
$^{27}\text{Na} + ^{244}\text{Pu} \rightarrow ^{263}\text{Lr} + \alpha 4n$	50.9	19.0	9.8×10^{-6}	88
$^{21}\text{O} + ^{249}\text{Bk} \rightarrow ^{264}\text{Lr} + \alpha 2n$	40.8	6.8	1.4×10^{-6}	9.8
$^{23}\text{F} + ^{248}\text{Cm} \rightarrow ^{264}\text{Lr} + \alpha 3n$	46.1	17.2	6.7×10^{-6}	110
$^{27}\text{Na} + ^{244}\text{Pu} \rightarrow ^{264}\text{Lr} + \alpha 3n$	47.0	10.5	5.5×10^{-6}	27
$^{23}\text{F} + ^{248}\text{Cm} \rightarrow ^{265}\text{Lr} + \alpha 2n$	40.8	3.0	1.2×10^{-6}	3.7
$^{27}\text{Na} + ^{244}\text{Pu} \rightarrow ^{265}\text{Lr} + \alpha 2n$	42.1	1.8	6.9×10^{-7}	0.6
$^{20}\text{O} + ^{248}\text{Cm} \rightarrow ^{263}\text{Rf} + 5n$	46.4	30.3	2.4×10^{-6}	72
$^{20}\text{O} + ^{248}\text{Cm} \rightarrow ^{264}\text{Rf} + 4n$	38.7	3.7	2.6×10^{-5}	95
$^{21}\text{O} + ^{248}\text{Cm} \rightarrow ^{264}\text{Rf} + 5n$	43.6	18.2	1.7×10^{-5}	310
$^{20}\text{O} + ^{248}\text{Cm} \rightarrow ^{266}\text{Rf} + 2n$	17.7	1.5×10^{-4}	3.8×10^{-2}	5.8
$^{21}\text{O} + ^{248}\text{Cm} \rightarrow ^{266}\text{Rf} + 3n$	24.6	3.9×10^{-3}	7.1×10^{-3}	27
$^{25}\text{Ne} + ^{248}\text{Cm} \rightarrow ^{266}\text{Rf} + \alpha 3n$	44.3	17.0	2.4×10^{-6}	40
$^{26}\text{Ne} + ^{248}\text{Cm} \rightarrow ^{266}\text{Rf} + \alpha 4n$	50.5	23.9	2.5×10^{-6}	59
$^{30}\text{Mg} + ^{244}\text{Pu} \rightarrow ^{266}\text{Rf} + \alpha 4n$	50.9	17.5	2.4×10^{-6}	16
$^{21}\text{O} + ^{248}\text{Cm} \rightarrow ^{268}\text{Rf} + 1n$	10.7	4.7×10^{-6}	3.7×10^{-1}	1.7
$^{26}\text{Ne} + ^{248}\text{Cm} \rightarrow ^{268}\text{Rf} + \alpha 2n$	40.4	6.0	1.8×10^{-7}	1.1
$^{20}\text{O} + ^{249}\text{Bk} \rightarrow ^{264}\text{Db} + 5n$	45.9	29.4	2.4×10^{-6}	72
$^{21}\text{F} + ^{248}\text{Cm} \rightarrow ^{264}\text{Db} + 5n$	48.2	14.8	1.6×10^{-6}	23
$^{25}\text{Na} + ^{244}\text{Pu} \rightarrow ^{264}\text{Db} + 5n$	48.9	9.2	1.3×10^{-6}	7.7
$^{20}\text{O} + ^{249}\text{Bk} \rightarrow ^{265}\text{Db} + 4n$	37.9	2.9	5.4×10^{-5}	160
$^{21}\text{O} + ^{249}\text{Bk} \rightarrow ^{265}\text{Db} + 5n$	43.3	15.5	2.0×10^{-5}	300
$^{21}\text{F} + ^{248}\text{Cm} \rightarrow ^{265}\text{Db} + 4n$	38.9	3.2×10^{-1}	3.4×10^{-5}	11
$^{23}\text{F} + ^{248}\text{Cm} \rightarrow ^{269}\text{Db} + 2n$	17.2	3.4×10^{-5}	6.4×10^{-2}	2.2
$^{20}\text{O} + ^{251}\text{Cf} \rightarrow ^{267}\text{Sg} + 4n$	40.3	8.2	3.0×10^{-6}	24
$^{21}\text{O} + ^{249}\text{Cf} \rightarrow ^{267}\text{Sg} + 5n$	49.6	30.8	5.7×10^{-8}	1.7
$^{21}\text{O} + ^{250}\text{Cf} \rightarrow ^{267}\text{Sg} + 4n$	40.3	5.6	3.6×10^{-6}	20
$^{21}\text{O} + ^{251}\text{Cf} \rightarrow ^{267}\text{Sg} + 3n$	28.7	1.5×10^{-2}	1.9×10^{-4}	2.8
$^{24}\text{Ne} + ^{248}\text{Cm} \rightarrow ^{267}\text{Sg} + 5n$	46.2	19.0	1.3×10^{-6}	24
$^{21}\text{O} + ^{249}\text{Cf} \rightarrow ^{268}\text{Sg} + 4n$	41.8	4.8	1.3×10^{-6}	6.2
$^{24}\text{Ne} + ^{248}\text{Cm} \rightarrow ^{268}\text{Sg} + 4n$	38.2	1.4	2.6×10^{-5}	37
$^{25}\text{Ne} + ^{248}\text{Cm} \rightarrow ^{268}\text{Sg} + 5n$	43.1	13.4	7.3×10^{-6}	98
$^{26}\text{Ne} + ^{248}\text{Cm} \rightarrow ^{270}\text{Sg} + 4n$	37.9	2.2	8.5×10^{-6}	19
$^{30}\text{Mg} + ^{244}\text{Pu} \rightarrow ^{270}\text{Sg} + 4n$	37.6	4.7×10^{-1}	1.6×10^{-5}	2.5
$^{26}\text{Ne} + ^{248}\text{Cm} \rightarrow ^{272}\text{Sg} + 2n$	17.3	1.0×10^{-4}	1.8×10^{-3}	0.2

Among all fusion-evaporation reactions presented, the reactions $^{20}\text{O} + ^{251}\text{Cf} \rightarrow ^{267}\text{Sg} + 4n$, $^{24}\text{Ne} + ^{248}\text{Cm} \rightarrow ^{267,268}\text{Sg} + 5n, 4n$, $^{25}\text{Ne} + ^{248}\text{Cm} \rightarrow ^{268}\text{Sg} + 5n$, and $^{26}\text{Ne} + ^{248}\text{Cm} \rightarrow ^{270}\text{Sg} + 4n$ seem to be the optimal ones for producing new isotopes $^{267,268,270}\text{Sg}$ with the following cross sections: $\sigma_{4n}(^{267}\text{Sg}) = 24$ nb, $\sigma_{5n}(^{267}\text{Sg}) = 24$ nb, $\sigma_{5n}(^{268}\text{Sg}) = 98$ nb, $\sigma_{4n}(^{268}\text{Sg}) = 37$ nb, and $\sigma_{4n}(^{270}\text{Sg}) = 19$ nb.

IV. SUMMARY

The production cross sections of new isotopes $^{261,263,264}\text{No}$, $^{263-265}\text{Lr}$, $^{263,264,266,268}\text{Rf}$, $^{264,265,269}\text{Db}$, and $^{267,268,270,272}\text{Sg}$ in the αxn and xn evaporation channels of the asymmetric hot fusion reactions with the radioactive beams were predicted within the DNS model. It was shown that the charged particle evaporation channels are suitable for producing these unknown isotopes with the cross sections of about 0.1–300 nb. The

optimal reactions and charge particle evaporation channels for the production of new isotopes were proposed. Thus, employing the reactions suggested, one can fill a gap of unknown isotopes between the isotopes obtained in the neutron evaporation channels of the lead- and bismuth-based cold and actinide-based hot fusion reactions. With the cross sections predicted the intensities of the radioactive beams can be up to 10^5 times smaller than those for the stable beams to supply the suitable production rates.

ACKNOWLEDGMENTS

This work is supported by the Rare Isotope Science Project of Institute for Basic Science funded by Ministry of Science, ICT and Future Planning and National Research Foundation of Korea (2013M7A1A1075764). G.G.A. and N.V.A. acknowledge the partial support of the Russian Foundation for Basic Research (Moscow) and the DFG (Bonn). The research was partly supported by a Tomsk Polytechnic University Competitiveness Enhancement Program grant.

-
- [1] Yu. Ts. Oganessian, *J. Phys. G* **34**, R165 (2007).
- [2] Y. T. Oganessian *et al.*, *Phys. Rev. Lett.* **104**, 142502 (2010); *Phys. Rev. C* **87**, 014302 (2013); **87**, 034605 (2013); **87**, 054621 (2013); V. K. Utyonkov *et al.*, *ibid.* **92**, 034609 (2015).
- [3] Y. T. Oganessian and V. K. Utyonkov, *Nucl. Phys. A* **944**, 62 (2015).
- [4] R. Eichler *et al.*, *Nature (London)* **447**, 72 (2007).
- [5] S. Hofmann *et al.*, *Eur. Phys. J. A* **32**, 251 (2007).
- [6] L. Stavsetra, K. E. Gregorich, J. Dvorak, P. A. Ellison, I. Dragojevic, M. A. Garcia, and H. Nitsche, *Phys. Rev. Lett.* **103**, 132502 (2009).
- [7] C. E. Dullmann *et al.*, *Phys. Rev. Lett.* **104**, 252701 (2010).
- [8] J. M. Gates *et al.* *Phys. Rev. C* **83**, 054618 (2011).
- [9] S. Hofmann *et al.*, *Eur. Phys. J. A* **48**, 62 (2012).
- [10] J. M. Khuyagbaatar *et al.*, *Phys. Rev. Lett.* **112**, 172501 (2014).
- [11] S. Hofmann *et al.*, *Eur. Phys. J. A* **52**, 180 (2016).
- [12] S. Hofmann and G. Münzenberg, *Rev. Mod. Phys.* **72**, 733 (2000).
- [13] K. Morita *et al.*, *Eur. Phys. J. A* **21**, 257 (2004); *J. Phys. Soc. Jpn.* **73**, 2593 (2004); **76**, 043201 (2007).
- [14] J. Peter *et al.*, *Nucl. Phys. A* **734**, 192 (2004).
- [15] S. Hofmann, *Lect. Notes Phys.* **764**, 203 (2009); **99**, 405 (2011).
- [16] G. G. Adamian, N. V. Antonenko, and A. S. Zubov, *Phys. Rev. C* **71**, 034603 (2005).
- [17] V. V. Volkov, *Phys. Rep.* **44**, 93 (1978); *Nuclear Reactions of Deep Inelastic Transfers* (Energoizdat, Moscow, 1982).
- [18] W. U. Schröder and J. R. Huizenga, in *Treatise on Heavy-Ion Science*, edited by D. A. Bromley (Plenum Press, New York, 1984), Vol. 2, p.115.
- [19] R. T. de Souza, J. R. Huizenga, and W. U. Schröder, *Phys. Rev. C* **37**, 1901 (1988); R. T. de Souza, W. U. Schröder, J. R. Huizenga, J. Toke, S. S. Datta, and J. L. Wile, *ibid.* **39**, 114 (1989).
- [20] V. V. Volkov, in *Treatise on Heavy-Ion Science*, edited by D. A. Bromley (Plenum Press, New York, 1989), Vol. 8, p. 255.
- [21] J. Randrup, *Nucl. Phys. A* **307**, 319 (1978); **327**, 490 (1979).
- [22] G. G. Adamian, A. K. Nasirov, N. V. Antonenko, and R. V. Jolos, *Phys. Part. Nucl.* **25**, 583 (1994).
- [23] Y. T. Oganessian (private communication).
- [24] J. Hong, G. G. Adamian, and N. V. Antonenko, *Phys. Rev. C* **94**, 044606 (2016).
- [25] W. Loveland, *Phys. Rev. C* **76**, 014612 (2007).
- [26] X. J. Bao, Y. Gao, J. Q. Li, and H. F. Zhang, *Phys. Rev. C* **91**, 064612 (2015).
- [27] J. Q. Li, C. Li, G. Zhang, L. Zhu, Z. Liu, and F.-S. Zhang, *Phys. Rev. C* **95**, 054612 (2017).
- [28] N. V. Antonenko, E. A. Cherepanov, A. K. Nasirov, V. B. Permjakov, and V. V. Volkov, *Phys. Lett. B* **319**, 425 (1993); *Phys. Rev. C* **51**, 2635 (1995).
- [29] G. G. Adamian, N. V. Antonenko, W. Scheid, and V. V. Volkov, *Nucl. Phys. A* **633**, 409 (1998); *Nuovo Cimento A* **110**, 1143 (1997).
- [30] G. G. Adamian, N. V. Antonenko, and W. Scheid, *Nucl. Phys. A* **678**, 24 (2000).
- [31] G. G. Giardina, S. Hofmann, A. I. Muminov, and A. K. Nasirov, *Eur. Phys. J. A* **8**, 205 (2000); G. G. Giardina, F. Hanappe, A. I. Muminov, A. K. Nasirov, and L. Stuttgé, *Nucl. Phys. A* **671**, 165 (2000); A. K. Nasirov *et al.*, *ibid.* **759**, 342 (2005); H. Q. Zhang, C. L. Zhang, C. J. Lin, Z. H. Liu, F. Yang, A. K. Nasirov, G. Mandaglio, M. Manganaro, and G. Giardina, *Phys. Rev. C* **81**, 034611 (2010); A. K. Nasirov, G. Mandaglio, G. G. Giardina, A. Sobiczewski, and A. I. Muminov, *ibid.* **84**, 044612 (2011).
- [32] Z. H. Liu and J. D. Bao, *Phys. Rev. C* **74**, 057602 (2006).
- [33] N. Wang, J. Tian, and W. Scheid, *Phys. Rev. C* **84**, 061601(R) (2011).
- [34] N. Wang, E. G. Zhao, W. Scheid, and S. G. Zhou, *Phys. Rev. C* **85**, 041601(R) (2012); N. Wang, E. G. Zhao, and W. Scheid, *ibid.* **89**, 037601 (2014).
- [35] L. Zhu, Z. Q. Feng, C. Li, and F. S. Zhang, *Phys. Rev. C* **90**, 014612 (2014); Z. Q. Feng, G. M. Jin, J. Q. Li, and W. Scheid, *ibid.* **76**, 044606 (2007).
- [36] A. S. Zubov, G. G. Adamian, N. V. Antonenko, S. P. Ivanova, and W. Scheid, *Phys. Rev. C* **68**, 014616 (2003).
- [37] G. G. Adamian, N. V. Antonenko, W. Scheid, and A. S. Zubov, *Phys. Rev. C* **78**, 044605 (2008).
- [38] G. G. Adamian, N. V. Antonenko, and W. Scheid, *Clustering Effects Within the Dinuclear Model*, in *Lecture Notes in Physics*, edited by Christian Beck, 848, 165 (2012).
- [39] J. Hong, G. G. Adamian, and N. V. Antonenko, *Phys. Rev. C* **92**, 014617 (2015); *Eur. Phys. J. A* **52**, 305 (2016); *Phys. Lett. B* **764**, 42 (2017).
- [40] V. S. Barashenkov and V. D. Toneev, *High Energy Interaction of Particles and Nuclei with Atomic Nuclei* (Atomizdat, Moscow, 1972).
- [41] R. Vandenbosch and J. R. Huizenga, *Nuclear Fission* (Academic Press, New York, 1973).
- [42] A. Ignatyuk, *Statistical Properties of Excited Atomic Nuclei* (Energoatomizdat, Moscow, 1983).
- [43] E. A. Cherepanov, A. S. Iljinov, and M. V. Mebel, *J. Phys. G: Nucl. Phys.* **9**, 931 (1983).

- [44] K. H. Schmidt and W. Morawek, [Rep. Prog. Phys.](#) **54**, 949 (1991).
- [45] A. S. Iljinov *et al.*, [Nucl. Phys. A](#) **543**, 517 (1992).
- [46] A. S. Zubov, G. G. Adamian, N. V. Antonenko, S. P. Ivanova, and W. Scheid, [Phys. Rev. C](#) **65**, 024308 (2002).
- [47] S. G. Mashnik, A. J. Sierk, and K. K. Gudima, [arXiv:nucl-th/0208048](#).
- [48] P. Möller, J. R. Nix, W. D. Myers, and W. J. Swiatecki, [At. Data Nucl. Data Tables](#) **59**, 185 (1995).
- [49] G. G. Adamian *et al.*, [Int. J. Mod. Phys. E](#) **5**, 191 (1996).
- [50] A. J. Sierk, [Phys. Rev. C](#) **33**, 2039 (1986).